VOLUME 101 | SUPPLEMENT 1 | MARCH 2021

LI

LABORATORY INVESTIGATION

THE BASIC AND TRANSLATIONAL PATHOLOGY RESEARCH JOURNAL

ABSTRACTS

CARDIOVASCULAR PATHOLOGY (148-157)

MARCH 13-18, 2021 | VIRTUAL AND INTERACTIVE

Published by
SPRINGER NATURE
www.ModernPathology.org

USCAP
Creating a Better Pathologist
AN OFFICIAL JOURNAL OF THE UNITED STATES AND CANADIAN ACADEMY OF PATHOLOGY

EDUCATION COMMITTEE

Jason L. Hornick
Chair

Rhonda K. Yantiss, Chair
Abstract Review Board and Assignment Committee

Kristin C. Jensen
Chair, CME Subcommittee

Laura C. Collins
Interactive Microscopy Subcommittee

Raja R. Seethala
Short Course Coordinator

Ilan Weinreb
Subcommittee for Unique Live Course Offerings

David B. Kaminsky
(Ex-Officio)
Zubair W. Baloch
Daniel J. Brat
Sarah M. Dry
William C. Faquin
Yuri Fedoriw
Karen Fritchie
Jennifer B. Gordetsky
Melinda Lerwill
Anna Marie Mulligan
Liron Pantanowitz
David Papke,
Pathologist-in-Training
Carlos Parra-Herran
Rajiv M. Patel
Deepa T. Patil
Charles Matthew Quick
Lynette M. Sholl
Olga K. Weinberg
Maria Westerhoff
Nicholas A. Zoumberos,
Pathologist-in-Training

ABSTRACT REVIEW BOARD

Benjamin Adam
Rouba Ali-Fehmi
Daniela Allende
Ghassan Allo
Isabel Alvarado-Cabrero
Catalina Amador
Tatjana Antic
Roberto Barrios
Rohit Bhargava
Luiz Blanco
Jennifer Boland
Alain Borczuk
Elena Brachtel
Marilyn Bui
Eric Burks
Shelley Caltharp
Wenqing (Wendy) Cao
Barbara Centeno
Joanna Chan
Jennifer Chapman
Yunn-Yi Chen
Hui Chen
Wei Chen
Sarah Chiang
Nicole Cipriani
Beth Clark
Alejandro Contreras
Claudiu Cotta
Jennifer Cotter
Sonika Dahiya
Farbod Darvishian
Jessica Davis
Heather Dawson
Elizabeth Demicco
Katie Dennis
Anand Dighe
Suzanne Dintzis
Michelle Downes
Charles Eberhart
Andrew Evans
Julie Fanburg-Smith
Michael Feely
Dennis Firchau
Gregory Fishbein
Andrew Folpe
Larissa Furtado
Billie Fyfe-Kirschner
Giovanna Giannico
Christopher Giffith
Anthony Gill
Paula Ginter
Tamar Giorgadze
Purva Gopal
Abha Goyal
Rondell Graham
Alejandro Gru
Nilesh Gupta
Mamta Gupta
Gillian Hale
Suntrea Hammer
Malini Harigopal
Douglas Hartman
Kammi Henriksen
John Higgins
Mai Hoang
Aaron Huber
Doina Ivan
Wei Jiang
Vickie Jo
Dan Jones
Kirk Jones
Neerja Kambham
Dipti Karamchandani
Nora Katabi
Darcy Kerr
Francesca Khani
Joseph Khoury
Rebecca King
Veronica Klepeis
Christian Kunder
Steven Lagana
Keith Lai
Michael Lee
Cheng-Han Lee
Madelyn Lew
Faqian Li
Ying Li
Haiyan Liu
Xiuli Liu
Lesley Lomo
Tamara Lotan
Sebastian Lucas
Anthony Magliocco
Kruti Maniar
Brock Martin
Emily Mason
David McClintock
Anne Mills
Richard Mitchell
Neda Moatamed
Sara Monaco
Atis Muehlenbachs
Bita Naini
Dianna Ng
Tony Ng
Michiya Nishino
Scott Owens
Jacqueline Parai
Avani Pendse
Peter Pytel
Stephen Raab
Stanley Radio
Emad Rakha
Robyn Reed
Michelle Reid
Natasha Rekhtman
Jordan Reynolds
Andres Roma
Lisa Rooper
Avi Rosenberg
Esther (Diana) Rossi
Souzan Sanati
Gabriel Sica
Alexa Siddon
Deepika Sirohi
Kalliopi Siziopikou
Maxwell Smith
Adrian Suarez
Sara Szabo
Julie Teruya-Feldstein
Khin Thway
Rashmi Tondon
Jose Torrealba
Gary Tozbikian
Andrew Turk
Evi Vakiani
Christopher VandenBussche
Paul VanderLaan
Hannah Wen
Sara Wobker
Kristy Wolniak
Shaofeng Yan
Huihui Ye
Yunshin Yeh
Anjana Yeldandi
Gloria Young
Lei Zhao
Minghao Zhong
Yaolin Zhou
Hongfa Zhu

To cite abstracts in this publication, please use the following format: **Author A, Author B, Author C, et al. Abstract title (abs#). In "File Title."** ***Laboratory Investigation*** **2021; 101 (suppl 1): page#**

148 The Incidence and Molecular Characteristics of Sudden Cardiac Death in Eastern Ontario Regional Forensic Pathology Unit

Adrian Agostino[1], Alfredo Walker[2], John Veinot[3], Vidhya Nair[1]
[1]University of Ottawa, Ottawa, Canada, [2]Ottawa Hospital, University of Ottawa, Ottawa, Canada, [3]Ottawa Hospital, Ottawa, Canada

Disclosures: Adrian Agostino: None; Alfredo Walker: None; John Veinot: None; Vidhya Nair: None

Background: Sudden cardiac death (SCD) is a devastating outcome of a number of underlying cardiovascular diseases. While coronary artery disease is the most common cause of SCD, inherited cardiac disorders comprise a substantial proportion of SCD cases, including primary arrhythmogenic disorders and inherited cardiomyopathies. In 30% of SCD, no anatomical cause of death is identified at autopsy and in these cases, targeted genetic testing of DNA extracted from postmortem tissues may identify a gene mutation that either codes for an arrhythmogenic condition or cardiomyopathy. Findings from targeted molecular studies can provide an explanation for SCD and can also have implications for surviving first degree relatives with implementation of preventive strategies. Most times, however, variants of uncertain clinical significance are obtained for which no clear clinical action is indicated.

Design: This is a single center retrospective pathology study. Postmortem examination reports of all consecutive sudden deaths in the Eastern Ontario Forensic Unit, from August 2017 to August 2020 were reviewed. Deaths categorized as sudden cardiac death were counted and cases for targeted molecular pathology testing were extracted. A unique identifier was given to each case. Patient demographics were noted. The results of the molecular tests were reviewed and analyzed for observable trends.

Results: From August 2017 to August 2020, the Ottawa Forensics Unit had a total of 212 sudden cardiac death cases. 29 cases with no anatomic cause of death were sent for molecular analysis which resulted in 2 cases with known genetic variants, 18 cases with variants of undetermined significance and 9 negative cases. 29 different variants of undetermined significance were identified with the most common being MYOM1, SCN10A, FLNC, and MYH7.

Conclusions: The findings of our study reiterate the importance of requesting postmortem cardiac genetic analysis in cases of sudden cardiac death with no anatomic cause of death. In the two cases with known genetic variants, the relatives were recommended further testing and clinical follow up. No further workup was recommended for the 9 negative cases. The 18 cases with variants of undermined significance have to be interpreted with caution, as there are no clinical guidelines available. Hopefully, the optimization of genomic data management will increase reference clinical databases and will help to reclassify these variants into specific pathological classes and guide clinical management.

149 Missed Diagnosis of Cardiac Amyloidosis in Patients with Coronary Artery Bypass Surgery

Derald Charles[1], Alexis Musick[2], Carolyn Glass[3]
[1]Duke University Health System, Durham, NC, [2]Duke University School of Medicine, Durham, NC, [3]Duke University Medical Center, Durham, NC

Disclosures: Derald Charles: None; Alexis Musick: None; Carolyn Glass: None

Background: Amyloidosis results from pathologic extracellular deposition of a protein precursor into antiparallel peptide polymer beta-pleated sheets that are resistant to enzymatic degradation, resulting in life threatening end organ damage. Thirty-six precursor proteins have been deemed pathologic, of which multiple can affect the heart. Amyloid deposition can occur in the endocardium, myocardium (interstitial) as well as the vasculature, which can lead to infarction through coronary artery stenosis, heart failure via decreased myocardial compliance, and sudden cardiac death by electromechanical dissociation.

Design: We retrospectively reviewed available medical records (clinical course, imaging, and previous pathology diagnosis) of decedents diagnosed at autopsy with amyloidosis and had undergone multi-vessel coronary artery bypass grafting (CABG) for severe coronary artery disease (CAD) over the past 20 years (2000-2020) at our institution.

Results: In our cohort of 14 decedents status-post CABG, amyloidosis was undiagnosed prior to autopsy in at least 13 of the cases (93% male, mean age at time of CABG 66, mean age at death 81). The majority of the decedents were clinically followed for a diagnosis of CAD (13/14), of which a subset (10/14) was treated for subsequent heart failure. Additionally, 7 decedents had diagnoses of arrythmias, and 1 decedent had a monoclonal gammopathy of undetermined significance. At autopsy, CAD was confirmed in all cases, 8 cases of which also had amyloid deposition within the coronary arteries. The pattern of amyloid deposition included vascular only (2/14), interstitial only (6/14) and combined vascular with interstitial (6/14). Half of the cases identified demonstrated severe interstitial involvement, of which the majority (5/7) had a clinical diagnosis of heart failure with corresponding echocardiographic imaging.

Figure 1 - 149

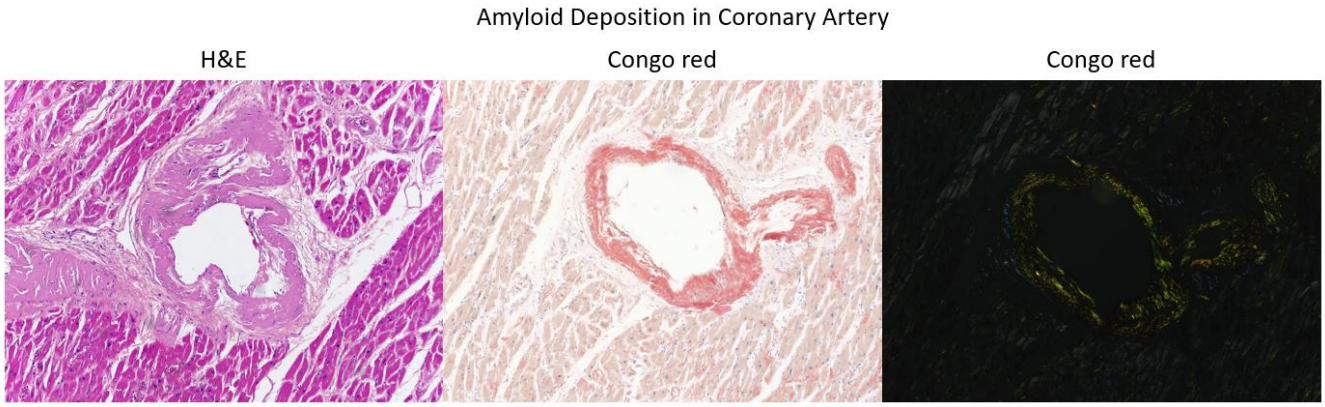

Conclusions: We have identified a cohort that, despite extensive cardiovascular workup and treatment, was not diagnosed with cardiovascular amyloidosis. These cases are a reminder that a diagnosis of CAD should not preclude a coinciding diagnosis of cardiac amyloidosis.

150 Morphologic and Molecular Cardiovascular Findings in COVID-19 Patients: A Single-Institution Autopsy Experience

Monica De Gaspari[1], Elisa Carturan[2], Mila Della Barbera[3], Cristina Basso[4], Stefania Rizzo[2]
[1]University of Padua, Padua, Italy, [2]University of Padua, Padova, Italy, [3]University of Padova, Padova, Italy, [4]University of Padua Medical School, Padova, Italy

Disclosures: Monica De Gaspari: None; Elisa Carturan: None; Mila Della Barbera: None; Cristina Basso: None; Stefania Rizzo: None

Background: Coronavirus 2 (SARS-CoV-2) primarily cause pulmonary damage but patients present multiorgan dysfunction that contribute to death. The study aims to describe the main cardiovascular features in the novel coronavirus disease (COVID-19) victims.

Design: From March to July 2020, postmortem analysis of people deceased from COVID-19 confirmed by nasopharyngeal swab was performed in a tertiary referral hospital, together with review of the clinical and laboratory data. Immunostains to characterize the inflammatory response were used. RT-PCR (nucleocapsid protein gene followed by ORF gene assay), transmission electron microscopy (TEM) and in situ hybridization for SARS-CoV-2 were carried out on post-mortem samples.

Results: Forty-one consecutive patients, mean age 81.4±12.7-year-old (range 58-97), 22 (54%) males were investigated. The average interval from symptom onset to death was 4.7 days (range 1-26 days). All patients had at least one cardiovascular risk factor (diabetes mellitus, smoking, hypertension, dyslipidemia). The mean cardiac troponin level was 1680.7±6571.2 ng/L (range 37-30345, NV 0-34 ng/L). Acute respiratory distress syndrome was the primary cause of death in 28 (68%) patients, characterized by diffuse alveolar damage and microthrombosis. Cardiovascular disease (ischemic heart disease, cardiac amyloidosis, dilated cardiomyopathy, valvular heart disease) and cancer contributed to death in 13 (32%) patients, 9 and 4 respectively. Cardiac involvement

manifested as pericarditis (n. 11), myocarditis (n. 2), endocardial thrombosis (n. 2). Microthrombosis was found in the myocardium in 8 (19.5%) cases. Increased inflammatory mononuclear cells with a mean number of 48/HPF macrophages (range 29-84) were found. Acute coronary plaque instability was never observed. In a subgroup of 26 patients assessed by RT-PCR, SARS-CoV-2 was identified in the lungs (19, 73%), myocardium (12, 46%) and kidneys (9, 34.6%). TEM failed to detect the virus in the myocytes. In situ hybridization in the myocarditis cases showed evidence of virus in the endothelial cells and macrophages but not in cardiac myocytes.

Conclusions: Inflammatory macrophagic response and microvasculature dysfunction represent the main cardiovascular findings in COVID-19 patients. Cardiovascular comorbidities are frequent in this elderly population. Molecular tools applied on tissue samples are crucial to assess the etiopathogenetic mechanisms of SARS-CoV-2 tissue damage.

151 Pathological and Clinical Associations of Cardiac Infection by SARS-CoV-2 in Patients Dying from COVID-19

Mayara Bearse[1], Yin Hung[1], Liana Bonanno[1], Baris Boyraz[1], Cynthia Harris[1], Timothy Helland[1], Caroline Hilburn[1], Bailey Hutchison[1], Soma Jobbagy[1], Michael S. Marshall[1], Dan Shepherd[1], Julian Villalba[2], Isabela Delfino[3], Javier Mendez-Pena[1], Ivan Chebib[2], Christopher Newton-Cheh[1], James Stone[1]
[1]Massachusetts General Hospital, Boston, MA, [2]Massachusetts General Hospital, Harvard Medical School, Boston, MA, [3]My Institution Is Not Listed, Brazil

Disclosures: Mayara Bearse: None; Yin Hung: None; Liana Bonanno: None; Baris Boyraz: None; Cynthia Harris: None; Timothy Helland: None; Caroline Hilburn: None; Bailey Hutchison: None; Soma Jobbagy: None; Michael S. Marshall: None; Dan Shepherd: None; Julian Villalba: None; Isabela Delfino: None; Javier Mendez-Pena: None; Ivan Chebib: None; Christopher Newton-Cheh: None; James Stone: None

Background: Both myocardial inflammation and myocarditis have been reported in patients dying from COVID-19; however, the underlying mechanisms responsible for these changes and the role of SARS-CoV-2 have not been established. The aim of this study was to determine the relationship between cardiac infection by SARS-CoV-2 and the presence of cardiac pathologic changes in a cohort of patients dying from COVID-19.

Design: Cardiac tissue from 41 patients dying from COVID-19 was analyzed, and the medical records were reviewed. Every patient had a nasopharyngeal swab positive for SARS-CoV-2. The presence of myocarditis and myocardial inflammation were identified on H&E-stained slides. The degree of inflammation was quantified on the tissue block with the most inflammatory cells using immunohistochemistry. The presence of SARS-CoV-2 in the heart was assessed by *in-situ* hybridization with virus$^+$ cases showing elevated levels of staining compared with controls.

Results: SARS-CoV-2 was observed in the hearts of 30/41 (73%) cases: virus$^+$ with myocarditis (n=4), virus$^+$ without myocarditis (n=26), and virus$^-$ without myocarditis (n=11). The virus$^+$ cases demonstrated a median of 1.2 SARS-CoV-2$^+$ cells/cm^2 (range= 0.4-7.4). Compared with virus$^-$ cases, virus$^+$ cases showed increased levels of cells staining for CD68 (P=0.01), CD3 (P=0.02) and CD4 (P=0.02). Compared with non-myocarditis cases, myocarditis cases showed increased staining for CD68, CD3 and CD4. The SARS-CoV-2$^+$ cells consisted predominantly of interstitial cells, consistent with macrophages, as well as rare endothelial cells and myocytes. CD61$^+$ microthrombi were present in 3/8 (38%) cases with virus$^+$ endothelial cells compared with 2/33 (6%) cases without virus$^+$ endothelial cells (P=0.04). Myocarditis was present in 3/6 (50%) cases with virus$^+$ myocytes, compared with 1/35 (3%) cases without virus$^+$ myocytes (P=0.007). Two of 3 (67%) patients treated with IL-6 blockade demonstrated myocarditis, compared with 0/14 patients treated with non-biologic immunosuppression (NBI), primarily glucocorticoids (P=0.02). Cardiac infection by SARS-CoV-2 was seen in 7/14 (50%) patients treated with NBI, compared with 21/24 (88%) patients who did not receive NBI (P=0.02).

Conclusions: In patients dying from COVID-19, myocarditis and myocardial microthrombi are associated with SARS-CoV-2 infection of myocytes and endothelial cells, respectively. Non-biologic immunosuppression is associated with lower incidence of myocarditis and cardiac infection by SARS-CoV-2.

152 Proteins Associated with Systemic Disease Are Detected in Clinically Unsuspected Isolated Amyloidosis in Atrial Appendages and Cardiac Valves

Jose Manuel Gutierrez Amezcua[1], Fang Zhou[2], Andre Moreira[3], Navneet Narula[3]
[1]New York University Medical Center, New York, NY, [2]NYU School of Medicine, New York, NY, [3]NYU Langone Health, New York, NY

Disclosures: Jose Manuel Gutierrez Amezcua: None; Fang Zhou: None; Andre Moreira: None; Navneet Narula: None

Background: Cardiac amyloidosis may occur as part of a systemic process or as a localized pathology. Isolated atrial amyloidosis (IAA) is of uncertain clinical significance, increases with age, and comprises alpha-atrial natriuretic peptide (AANF), a protein synthesized by atrial myocytes. Isolated valvular amyloid deposits in surgically excised valves are considered to be incidental with no clinical significance.

We evaluated the clinical relevance of characterization of incidentally detected amyloid in surgically excised atrial appendages and cardiac valves by liquid chromatography tandem mass spectrometry (LC-MS/MS).

Design: Atrial appendages and valves with a diagnosis of amyloidosis were identified retrospectively in our database from March 2018 to October 2020.

Results: Clinically unsuspected amyloid was identified in 55 specimens, including 17 atrial appendages and 38 valves. LC-MS/MS typing of amyloid protein was available in 16 atrial appendages and 29 valves. In the 16 atrial appendages, 14 (87.5%) had AANF and 2 (12.5%) had transthyretin-type amyloid (ATTR). Of the 29 valves, 18 (62.1%) had indeterminate amyloid (serum amyloid P component, apolipoprotein A4 and apolipoprotein E), 3 (10.3%) had ATTR, and 2 (6.9%) cases had immunoglobulin (Ig)-associated amyloid; 1 case (3.4%) each had combined ATTR + AL (kappa light chain), AL (kappa light chain), and AH (mu heavy chain [μH]) amyloid. In the remaining 3 cases (10.3%) the amyloid was predominantly indeterminate type with small amount of ATTR. No amino acid abnormality was detected in any case of ATTR amyloid (Table 1). On clinical follow-up, one of the patients with ATTR on atrial appendage was found to have extensive cardiac involvement and is currently enrolled in a blinded clinical trial for symptomatic Transthyretin-Amyloid Cardiomyopathy.

Table 1: Proteins detected in incidental, isolated amyloidosis of atrial appendages and cardiac valves

Atrial appendages (n=16)	**n (%)**
AANF	14 (87.5%)
ATTR*+	2 (12.5%)
Cardiac valves (n=29)	**n (%)**
Indeterminate^	18 (62.1%)
ATTR*	3 (10.3%)
Indeterminate, low level ATTR	3 (10.3%)
Ig-associated	2 (6.9%)
ATTR and AL kappa	1 (3.4%)
AL kappa	1 (3.4%)
AH mu	1 (3.4%)

*All cases of ATTR were wild-type by LC-MS/MS

+ One case was subsequently diagnosed with Transthyretin-Amyloid Cardiomyopathy and is currently enrolled in a clinical trial.

^Indeterminate cases contained proteins deposited with amyloid of all types (serum amyloid P component, apolipoprotein A4, and apolipoprotein E), without the identification of a specific amyloid type.

Abbreviations: AANF=amyloid atrial natriuretic factor; ATTR=amyloid transthyretin; Ig=immunoglobulin; AL=amyloid light chain; AH=amyloid heavy chain

Conclusions: ATTR, Ig, AL, or AH were observed in 2 of 16 (12.5%) atrial appendages and 8 of 29 (27.5%) valves. These types of amyloid are usually associated with significant cardiac involvement or systemic disease, which warrants close clinical follow-up. With recent therapeutic advances, early identification of the type of amyloid protein could help improve prognosis at least in a subset of patients.

153 Amyloid Deposition in Surgically Resected Aortic Valves

Philip Hurst[1], Joseph Maleszewski[1], Ellen McPhail[1], Marie-Christine Aubry[1], Peter Lin[1], Ying-Chun Lo[1], Shareef Mansour[1], Martha Grogan[1], Omar AbouEzzeddine[1], Melanie Bois[1]
[1]Mayo Clinic, Rochester, MN

Disclosures: Philip Hurst: None; Joseph Maleszewski: None; Ellen McPhail: None; Marie-Christine Aubry: None; Peter Lin: None; Ying-Chun Lo: None; Shareef Mansour: None; Omar AbouEzzeddine: None; Melanie Bois: None

Background: Amyloid deposition is variably reported in aortic valves (AVs), with a frequency between 15% and 82% in published series. However, its true incidence, proteomic characteristics, and clinical significance remain unclear. A detailed assessment of surgically resected aortic valves was undertaken with the following aims: 1) employ robust methodology to further characterize AV amyloid incidence, 2) determine the proteomic signature of such deposits, and 3) investigate clinical importance of this finding.

Design: 100 consecutive surgically resected AVs (11/2018-2/2019) were identified through institutional records. Clinical material was semiquantitatively scored for the degree of calcium and inflammation present. Congo red (CR) histochemistry was performed to determine the presence and morphology of CR+ deposits. A subset of cases with adequate CR+ deposits underwent liquid chromatography-tandem mass spectrometry (LC-MS/MS) and electron microscopy. Relevant clinical information was abstracted from the medical record. Echocardiograms, including pre-operative and most recent (if different) were reviewed for features indicative of cardiac amyloidosis.

Results: Patient characteristics are presented in Table 1. Half (52%) of the resected AVs contained CR+ deposits. Patients with CR+ deposits were older (p=0.003), and more commonly men (p=0.047). Though non-specific sequelae of systemic amyloidosis were more common in this population (erectile dysfunction, p=0.029; carpal tunnel syndrome, p<0.0001), no significant difference was apparent on echocardiography and no patients were diagnosed with cardiac amyloid during the follow-up period. CR+ deposits were directly associated with calcium deposition (p<0.0001) and usually adjacent to it (65%), with 5 (10%) valves containing exclusively nodular deposits away from calcium, and 13 (25%) showing both morphologies. Proteomic analysis was performed on microdissected CR+ deposits from 9 cases, all revealing a universal amyloid protein signature. Pericalcific deposits show a non-specific proteome, while nodular deposits have a profile more typical of ATTR (transthyretin) amyloidosis. Ultrastructural and additional LC-MS/MS analysis is ongoing.

Table 1.

	Congo red-positive (n=52)	Congo red-negative (n=48)	p-value
Patient Characteristics			
Age (years), median (IQR)	67 (63, 74)	64 (51, 71)	0.0032
Sex, M (%)	37 (71)	31 (65)	0.0465
Follow up interval (days), median (IQR)	386 (195, 475)	471 (364, 580)	0.051
Erectile dysfunction (men), n (%)	14 (38)	8 (29)	0.0285
Carpal tunnel syndrome, n (%)	12 (24)	5 (11)	<0.0001
Valve Properties			
Valve status	43 (86)	25 (53)	

Stenotic Regurgitant NOS	1 (2) 6 (12)	21 (45) 1 (2)	
Histopathologic Diagnosis Degenerative fibrocalcific Congenitally bicuspid Post-inflammatory Annular dilatation	28 (54) 22 (43) 2 (4) -	18 (38) 17 (35) 2 (4) 11 (23)	
Calcium*, mean	2.42	1.19	<0.0001
Chronic inflammation*, mean	0.94	0.44	0.0001
Echocardiography Properties			
Septal wall thickness (mm), median (IQR)	13 (11, 14)	11 (10, 14)	0.3665
Posterior wall thickness (mm), median (IQR)	11.5 (10, 13)	11 (9.5, 12)	0.1915

*semi-quantitative: 0=none, 1=mild, 2=moderate, 3=marked

IQR= interquartile range; n=number

Conclusions: CR+ deposits are relatively common in AVs, specifically those in which there is concomitant fibrocalcific degeneration, and are associated with degree of calcification, older age, and male sex, in keeping with prior literature. However, morphologic differences are present, requiring correlation with proteomic and ultrastructural studies, as well as clinical outcome, to further characterize the nature of these deposits.

154 Age-Related Histopathologic Findings in Temporal Arteries Can Mimic Healed Arteritis

Ryan Kendziora[1], Melanie Bois[1], Marie-Christine Aubry[1], Ying-Chun Lo[1], Joseph Maleszewski[1], Peter Lin[1]
[1]Mayo Clinic, Rochester, MN

Disclosures: Ryan Kendziora: None; Melanie Bois: None; Marie-Christine Aubry: None; Ying-Chun Lo: None; Joseph Maleszewski: None; Peter Lin: None

Background: Histopathologic findings indicative of healed giant cell arteritis (GCA) include intimal fibroplasia (IF), disruption of the internal elastic lamina (IEL), medial attenuation (MA) and medial fibrosis (MF) . However, some of these findings may also occur secondary to age-related processes. To this end, autopsy-derived temporal arteries (TA) were systematically evaluated to characterize the spectrum of age-related findings.

Design: Bilateral TAs were sampled from the galeal surface of the scalp during consecutive autopsies. Serial sections of TAs were evaluated in a semi-quantitative fashion (0=none; 1=<10%; 2=10-50%; 3=>50% involvement) for each of the following categories: IF; disruption and calcification of the IEL; MA; MF and inflammation. Paired aortic specimens were reviewed. Salient clinical information was abstracted from the medical record. Results were compared to a positive control cohort of 16 patients with healed arteritis who had previous biopsy-proven active temporal arteritis within the preceding 12 months.

Results: 43 patients (mean age 66.5; range 27-93 years) without a history of giant cell arteritis underwent sampling to date, with bilateral TAs obtained in 32 cases, and unilateral TAs in 11 cases.

6 patients had a clinical history of rheumatologic disease, including rheumatoid arthritis (n=4), lupus/mixed connective tissue disease (n=1), and autoimmune encephalitis (n=1). No patients had active temporal arteritis; however 6 patients had features suspicious for healed GCA, including 2 with rheumatologic disease (Table 1).

None had features of active or healed aortitis, but adventitial inflammation was common in all age groups. IEL calcification increased with age group. (Table 1).

IF, IEL disruption and MA scores were higher with increasing age groups (Figure 1). MF was not present in any age group.

When compared to the healed arteritis cohort (Figure 2), the most significant differences were seen with MF and MA. IF involving >50% of lumen was more common in healed GCA, and IF involving <50% of lumen was more common as an age-related change.

Diagnostic Groups							
Age Group (years)	**Patients (n=)**	**Temporal arteries (n=)**	**Adventitial inflammation (n=,%)**	**IEL Calcification (n=,%)**	**Active GCA (n=)**	**Suspicious for healed GCA (n=)**	**Suspicious for healed GCA excluding rheumatologic disease pts (n=,%)**
<60	11	19	9 (47.4%)	0	0	0	0
60-69	14	21	12 (57.1%)	2 (9.5%)	0	2	0
70-79	10	19	17 (89.5%)	5 (26.3%)	0	1	1 (10%)
80+	8	16	14 (87.5%)	9 (56.3%)	0	3	3 (37.5%)

Figure 1 - 154

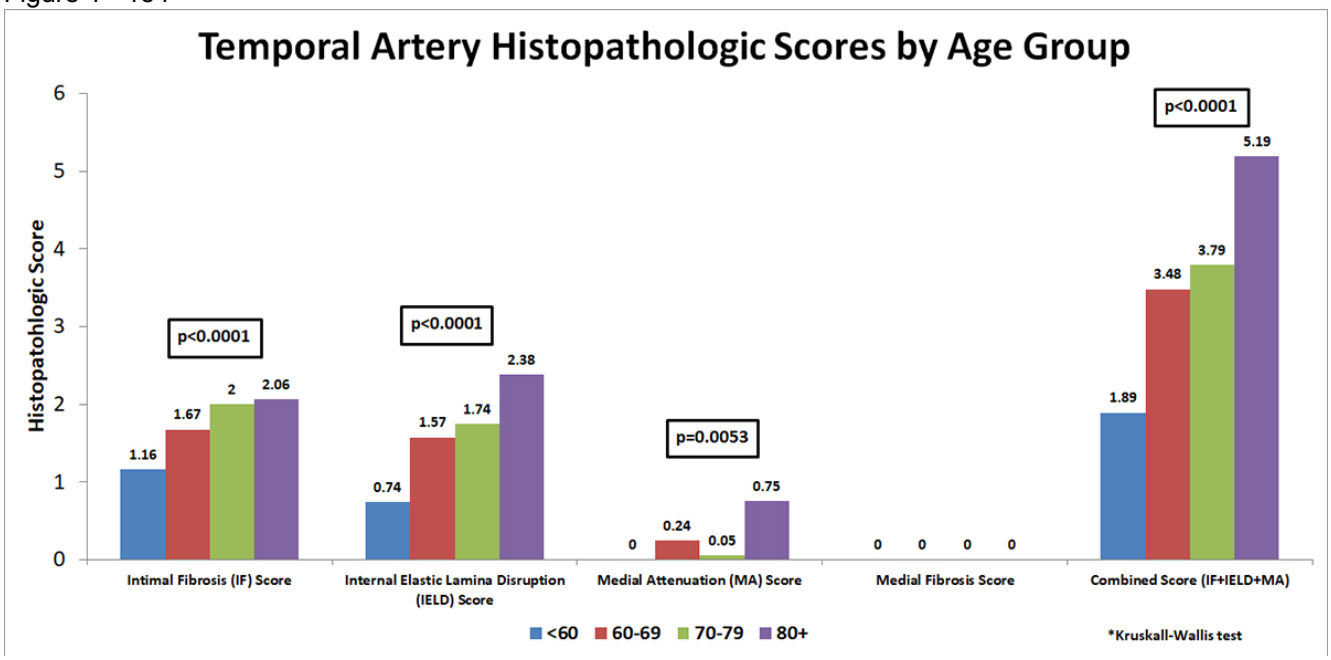

Figure 2 - 154

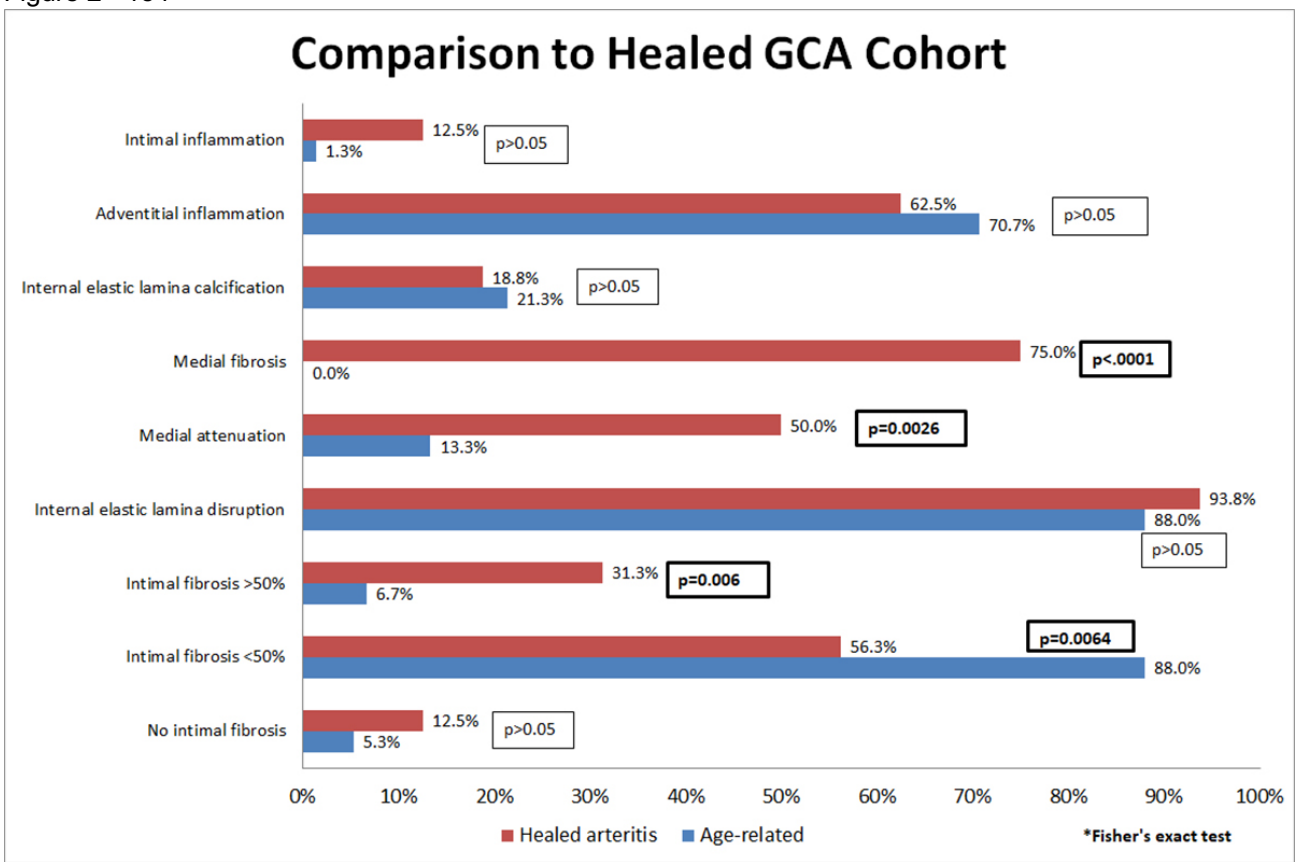

Conclusions: Age-related changes can mimic healed giant cell arteritis. Up to 37.5% of patients in the 80+ age group had histopathologic findings that were considered suspicious for healed arteritis. Therefore, consideration of the patient's age is warranted prior to rendering a diagnosis of healed GCA.

IF, IEL disruption, MA, periadventitial and adventitial inflammation and IEL calcification were more common with increasing age groups. The presence of medial fibrosis and attenuation may be useful for distinguishing healed GCA from age-related change. IEL disruption is a common finding in both age-related change and healed GCA, and should not be used as the sole diagnostic feature of healed GCA.

155 Exploring Potential Histopathologic Correlates of Primary Cardiac Graft Dysfunction

Daniel Manzoor[1], Lillian Benck[1], Evan Kransdorf[1], Daniel Luthringer[2]
[1]Cedars-Sinai Medical Center, Los Angeles, CA, [2]Cedars-Sinai Medical Center, West Hollywood, CA

Disclosures: Daniel Manzoor: None; Evan Kransdorf: None; Daniel Luthringer: None

Background: Primary cardiac graft dysfunction (PGD) is an unfortunate complication of orthotopic heart transplantation (OHT) characterized by perioperative ventricular dysfunction, frequently resulting in graft failure and death. The etiology is uncertain, and pathologic studies are lacking. Here we critically analyze cardiac tissue obtained from patients who experienced severe PGD in hopes of better understanding the etiology and/or pathophysiology.

Design: Cardiac tissue from patients who experienced severe PGD (defined by clinical criteria) obtained within 30 days of OHT was used to optimize the identification of relevant pathologic processes. Cases included donor heart (DH) explants (re-transplants), autopsies, and first endomyocardial biopsy (EMB) post-OHT. A control group consisted of EMBs from age- and sex-matched OHT patients who did not suffer from PGD. Detailed histopathologic analysis was performed and the presence of acute cellular rejection (ACR) and antibody-mediated rejection (AMR)

was determined using criteria defined by the International Society for Heart and Lung Transplantation (ISHLT). Immunohistochemical (IHC) stains for C4d, C3d, and CD68 were used to assess for AMR. C4d/C3d IHC was also used to assess myocardial damage. Cases were reviewed by 2 cardiac pathologists; agreement by both was used for ACR and AMR classification.

Results: Tissue from 26 cases of severe PGD was compiled from 2 cardiac explants (re-transplants), 4 autopsy hearts, and 20 first post-OHT EMBs. The mean time (days) from OHT to tissue retrieval for each group was 4.0, 13.3, and 13.0, respectively. All 6 cardiac resections showed areas of myofiber coagulative necrosis with contraction bands that ranged from focal to diffuse; 4 had significant intracellular calcium deposits and vascular thrombi. There was no evidence of ACR (of any grade) or AMR 2. Of the 20 PGD EMBs, 10 showed myofiber injury/necrosis by either morphology and/or C4d/C3d IHC. One case had ACR (grade 1R, ISHLT 2004) and 2 had AMR 2 (ISHLT 2013). The mean time post-OHT to retrieval in the control group (n=24) was 6.2 days. Of those 24 cases, 5 showed myofiber injury, 3 had ACR (grade 1R, ISHLT 2004), and 2 had AMR 2 (ISHLT 2013).

Conclusions: The pathologic features of severe cardiac PGD are characterized by myofiber injury including coagulative necrosis. These findings support acute myocardial injury as the etiology and do not indicate ACR or AMR involvement.

156 Histologic Features of Medial Degeneration in Ascending Aortic Aneurysms and Dissections

Joseph Mininni[1], Allen Burke[2]
[1]University of Maryland Medical Center, Baltimore, MD, [2]University of Maryland Medical School of Medicine, Baltimore, MD

Disclosures: Joseph Mininni: None; Allen Burke: None

Background: In 2016, guidelines were published by Halushka et.al in Cardiovascular Pathology to diagnose and classify medial degenerative changes, based on multiple histologic criteria. We used these criteria to determine which medial degeneration changes were more severe in ascending aortic dissections compared to ascending aortic aneurysms.

Design: A retrospective and prospective analysis of fifty-two ascending aortic specimens was performed. Seven patients had congenitally bicuspid or unicuspid valves, and 3 patients had hereditary connective tissue disease. 26 were excised for aortic dissection, and 26 were elective surgeries for aneurysm. H&E, Alcian blue and elastic stains were used to grade the following histologic parameters on a four-point scale: translamellar and intralamellar mucoid extracellular matrix accumulation (TL-MEMA and IL-MEMA), elastic fiber fragmentation (EFF), smooth muscle cell loss (SMCL), and laminar medial collapse (LMC). Ten non-aneurysmal aortas obtained at autopsy from patients without aortic disease were used as controls.

Results: A score of 2 or more of TL-MEMA, IL-MEMA, EFF, SMCL, and LMC was seen in 10%, 69%, and 96% of controls, aneurysm without dissection, and dissections, respectively. Statistical comparison revealed that EFF, SMCL, and IL-MEMA were significantly greater in diseased aortas (dissected or aneurysmal) and that only EFF was significantly increased in dissected vs. non-dissected aneurysms.

	Mean score			p-value	p-value
	Control	Aneurysms	Dissections	control vs. diseased	aneurysms v. dissections
EFF	0.1	0.6	2.6	.002	<.0001
SMC	0.5	1.5	1.6	.003	0.9
IL -MEMA	0.4	1.7	2.4	.0008	.06

Figure 1 - 156

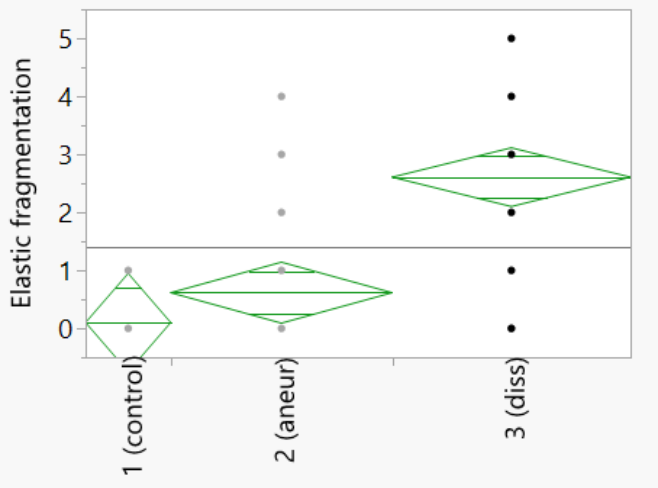

Conclusions: As expected, histologic abnormalities involving elastic tissue, smooth muscle cells, and accumulation of extracellular matrix are all increased in aortic aneurysms with or without dissection. Only elastic fragmentation is significantly increased in those aortas with dissection vs. non-dissected aneurysms, suggesting a role in pathogenesis.

157 Upregulation of Th2 Tolerance Profile in Heart Allografts with Quilty Lesions Suggests an Immunomodulatory Role

Samantha Moore[1], Qi Cai[1], Sakda Sathirareuangchai[1], Luis De Las Casas[1], Allen Hendricks[1], Jose Torrealba[1]
[1]UTSouthwestern Medical Center, Dallas, TX

Disclosures: Samantha Moore: None; Qi Cai: None; Sakda Sathirareuangchai: None; Luis De Las Casas: None; Allen Hendricks: None; Jose Torrealba: None

Background: Quilty lesions, lymphoid aggregates confined within endocardium or extending to subendocardium, are frequently encountered in heart allograft biopsies without morphologic evidence of rejection. However, their biologic nature and precise function remains unclear. Previously, in 42 cardiac allograft biopsies, we demonstrated that the presence of Foxp3+ innate and TGF-β+ adaptive regulatory lymphocytes in Quilty lesions are associated with higher allograft acceptance. In the current study, we aimed to characterize immunomodulatory pathways associated with Quilty lesions by measuring mRNA expression.

Design: Endomyocardial biopsies of heart allograft from nine patients were included in this study, four with unremarkable endomyocardium (control group) and five with at least one Quilty lesion (Quilty group). No acute T-cell or antibody mediated rejection was present histologically in any of these specimens. Total RNA was extracted from formalin fixed paraffin embedded tissue. Multiplexed mRNA measurement was performed using the nCounter system (NanoString Technologies, Seattle, WA), and data were analyzed with nSolver software (NanoString Technologies).

Results: Of 771 mRNA levels measured in the NanoString Transplant Immunology Panel, 274 were upregulated in the Quilty group over the control group, with approximately one third related to adaptive immunity and 5% to innate immunity. Higher levels of mRNA expression in the Quilty group were also shown in pathways for hematopoiesis (11%), cytokine (9%), chemokine (7%), cell-extracellular matrix interaction (7%), and apoptosis & cell cycle regulation (5%). More specifically, the mRNA expression of T_H2 tolerance-associated immunity markers, including Foxp3, TGF-β, and CTLA4, were higher in the Quilty group (2.82, 1.42, and 3.97 fold increase, respectively, with $p < 0.05$). Markers of rejection-associated T_H1 immunity, including IL-2 and IFN-g, although lower in the Quilty group, were not statistically different.

Conclusions: Heart allografts with Quilty lesions have dominant adaptive immunity related mRNA expression with significantly higher mRNA expression of T_H2 tolerant immunity markers. These data suggest that Quilty lesions, far from passive bystanders, may serve an immunomodulatory role in cardiac allografts. The presence of intra-allograft regulatory T-lymphocyte related signaling in Quilty lesions may help to reduce the risk of rejection and foster allograft acceptance.